

1 **Importance of biomass and binder selection for coking briquette preparation.**  
2 **Their effect on coal thermoplastic properties.**

3 L. Florentino-Madiedo<sup>a</sup>, E. Díaz-Faes<sup>a</sup>, C. Barriocanal<sup>a\*</sup>, M. Castro-Díaz<sup>b</sup>, C. E. Snape<sup>b</sup>

4 <sup>a</sup> Instituto Nacional del Carbón, INCAR-CSIC, Apartado 73, 33080 Oviedo, Spain

5 <sup>b</sup> Department of Chemical and Environmental Engineering, University of Nottingham,  
6 Nottingham NG7 2RD, United Kingdom

7 \*Corresponding author: carmenbr@incar.csic.es

8 **Abstract**

9 Blends consisting of a high volatile bituminous coal, biomass and binder that were used  
10 in the preparation of briquettes were analyzed in order to select the best components from  
11 the viewpoint of their influence on the coal's thermoplastic properties. The raw materials  
12 were studied by means of thermogravimetry, high-temperature rheometry, high-  
13 temperature proton nuclear magnetic resonance (<sup>1</sup>H NMR) and Fourier transform infrared  
14 (FTIR) spectroscopy. In addition, the fluidity of the blends was determined with the  
15 standard Gieseler plastometer test method (ASTM D 2639-74). Various parameters  
16 derived from these different techniques were used to explain the effects of biomass and  
17 binder on the fluidity of the blends with coal. It was found that the deleterious effect of  
18 biomass was mainly related to its physical properties, whereas the effect of the binder  
19 was controlled by its chemical composition. Coal tar, coal tar sludge, pine sawdust and a  
20 bio-coal derived from hydrothermally treated waste biomass obtained from pruning were  
21 the best materials for the preparation of briquettes for cokemaking.

22  
23 **Keywords**

24 Biomass, coal, binder, briquettes, fluidity.

25

26 **1. Introduction**

27 The use of additives has been common practice for many years in the cokemaking  
28 industry as a means to reduce costs, widen the range of raw materials that can be  
29 introduced into blends used for the preparation of metallurgical coke and recycle wastes  
30 produced in-situ and ex situ.<sup>1-6</sup>

31

32 In recent years, the use of biomass as an additive to coal blends, in order to produce  
33 metallurgical coke, has been envisaged as a possible solution for reducing the generation  
34 of non-renewable CO<sub>2</sub> emissions by the steel industry and for promoting the use of low-  
35 cost raw materials to replace expensive prime coking coals.<sup>7-9</sup> The direct addition of  
36 sawdust to industrial coal blends has been investigated but the resultant decrease in bulk  
37 density diminishes the quality of the coke.<sup>7</sup> It was also found that biomass produces a  
38 decrease in the fluidity of coal even at low addition levels of 0.75 wt%.

39

40 It has been proposed that the decrease in bulk density caused by the introduction of  
41 biomass in coal blends can be overcome with the use of briquettes. The quality of the  
42 coke produced from blends containing briquettes has been compared with the direct  
43 addition of un-briquetted components, with favorable results towards the use of  
44 briquettes.<sup>10</sup>

45

46 The use of coal tar as binder in the briquettes can compensate to some extent for the  
47 decrease in fluidity produced by the biomass. However, coal tar also leads to the  
48 formation of a large amount of polycyclic aromatic hydrocarbons (PAHs) during  
49 carbonization,<sup>11</sup> which are considered to be dangerous to human health by the US  
50 Environmental Protection Agency (EPA). Hence, in the present research work other

51 binders that are less pollutant, such as paraffin,<sup>12</sup> have been studied and compared with  
52 coal tar. Moreover, the thermoplastic properties of blends containing coal and biomass  
53 differ depending on the type of biomass used.<sup>13</sup> Therefore, four different biomass samples  
54 have been selected in this study in order to obtain a more comprehensive understanding  
55 of the mechanisms that control fluidity development in the blends.

56

57 Due to the importance of the coal plastic stage in the formation of the structure of coke,  
58 several conventional methods are currently used to measure coal thermoplasticity.  
59 Among these methods, the Gieseler<sup>14</sup> and Brabender<sup>15</sup> plastometers provide information  
60 about the softening, maximum fluidity and resolidification stages of coal. Novel  
61 techniques such as proton magnetic resonance thermal analysis (PMRTA)<sup>16</sup> and high-  
62 temperature <sup>1</sup>H NMR<sup>17</sup> have been used to measure the concentration and mobility of fluid  
63 hydrogen of carbonaceous materials during pyrolysis. High-temperature small-amplitude  
64 oscillatory-shear (SAOS) rheometry is another technique that can provide direct  
65 information about the viscoelastic properties of the bulk mass of coals in their  
66 thermoplastic temperature range.<sup>18</sup>

67

68 The aim of the present work is to determine the combination of biomass and binder that  
69 has the least deleterious effect on the thermoplastic properties of a low rank bituminous  
70 coal, and whenever possible, to correlate the results with the properties of the raw  
71 materials.

72

## 73 **2. Materials and Methods**

### 74 **2.1. Materials**

75 An American low rank bituminous coking coal with high volatile matter content (ca. 31.5  
76 wt%) and high Gieseler maximum fluidity (ca. 26000 ddpm) was used to prepare binary  
77 and ternary blends using eight different additives, namely four biomass wastes and four  
78 binders. The biomass samples were a pine sawdust obtained as waste from the timber  
79 industry (SP), the pine sawdust torrefied in a rotary oven of 95 mm diameter at 300 °C  
80 for half an hour under a 250 ml/min N<sub>2</sub> flow (SPT), pine Kraft lignin from the production  
81 of cellulose (Lg), and a commercial bio-coal derived from hydrothermally-treated waste  
82 biomass obtained from pruning (BIOC). The binders used included molasses from the  
83 sugar industry (Mol), paraffin (Par), coal tar (T) and coal tar sludge (CTS). T, CTS and  
84 Mol are liquids and Par is solid at room temperature. The bituminous binders T and CTS  
85 were obtained as by-products in an industrial coke plant. T was separated from the raw  
86 coke oven gas in the by-products plant and CTS was collected at the sole of the tar  
87 decanter. CTS not only contains tar and water but also fine particles of coal and coke,  
88 which are drawn away and deposited at the bottom of the tar decanter. Mol and CTS can  
89 be considered as waste materials while Par and T are commercial products. All these  
90 materials were characterized through proximate and ultimate analysis. Proximate analysis  
91 was carried out following the standard ISO 562 and ISO 1171 procedures for humidity,  
92 ash and volatile matter, respectively. Ultimate analysis was performed using the standard  
93 method ASTM D 5373-02 for the determination of C, H and N using a LECO CHN-2000  
94 instrument and the standard method ASTM D 5016-98 for the determination of S using a  
95 LECO S-144 DR instrument. The characteristics of the materials are presented in **Table**  
96 **1**. The maceral composition of the bituminous coal is as follows: 77.9% vitrinite, 8.4%  
97 liptinite, 8.0% semifusinite, 2.0% fusinite and 3.7% inertinite.

98

## 99 **2.2. Thermogravimetric analysis**

100 Thermogravimetric analysis (TGA) was carried out using a TA Instruments SDT  
101 2960 thermobalance. Approximately 10 mg of sample with a particle size < 0.212 mm were  
102 heated under a N<sub>2</sub> flow of 100 ml/min from room temperature to 1000 °C at a rate of 3  
103 °C/min.<sup>19</sup>

104

### 105 **2.3. Fourier transform infrared**

106 Fourier transform infrared (FTIR) spectra were recorded on a Nicolet Magna-IR560  
107 spectrometer equipped with a multi-bond ZnSe crystal attenuated total reflection (ATR)  
108 accessory and a DTGS detector. The spectra were collected over 128 scans at a resolution  
109 of 4 cm<sup>-1</sup> in the 4000–500 cm<sup>-1</sup> range. In order to facilitate comparison of the spectra,  
110 two semi-quantitative indices were defined (Table 2). The degree of aromaticity can be  
111 calculated by dividing the area of aromatic C–H groups ( $A_{ar}$ ) by the sum of the areas of  
112 aromatic and aliphatic C–H groups ( $A_{ar} + A_{al}$ ). However, some biomass samples did not  
113 present a visible peak for aromatic C–H groups (i.e.  $A_{ar} \approx 0$ ). Thus, the area of aromatic  
114 C=C groups ( $A_{C=C}$ ) divided by the area of aliphatic C–H groups ( $A_{al}$ ) was used instead to  
115 determine the degree of aromaticity of the samples.

116

### 117 **2.4. High-temperature <sup>1</sup>H nuclear magnetic resonance**

118 A Doty 200 MHz <sup>1</sup>H nuclear magnetic resonance (NMR) probe was used in conjunction  
119 with a Bruker MSL300 instrument to determine the development of fluidity in the raw  
120 materials. A detailed description of this technique has been published elsewhere.<sup>20</sup>  
121 Approximately 140–150 mg of sample (63–212 μm) was loosely packed inside a boron  
122 nitride container, and 100 scans were accumulated using a recycle delay of 0.3 s. All  
123 samples were analyzed at a heating rate of 3 °C/min. Spectra were acquired from 25 °C  
124 to 400 °C for the biomass samples, from 25 °C to 500 °C for the binders and from 360 °C

125 to 500 °C for the coal. The spectra were deconvoluted into Gaussian and Lorentzian  
126 distribution functions. The area of the Lorentzian peak multiplied by 100 and divided by  
127 the total area of the NMR signal represents the concentration of fluid H in the sample,  
128 and the width of the Lorentzian peak at half height is inversely proportional to the  
129 mobility of the fluid H or spin-spin relaxation time (T<sub>2L</sub>).

130

## 131 **2.5. High-temperature SAOS rheometry**

132 High-temperature small-amplitude oscillatory shear (SAOS) measurements were  
133 performed using a Rheometrics RDA-III high-torque controlled-strain rheometer<sup>21</sup>.  
134 Approximately 1.5 g of sample with a particle size of 63–212 μm were compacted with  
135 a hydraulic press under a 5-ton force to form discs of 25 mm in diameter. The biomass  
136 and coal samples, as well as the 95:5 wt/wt blends of coal with biomass and coal with  
137 binder were analyzed. Also, blends of coal pre-heated in N<sub>2</sub> to 466 °C (C466) with binder  
138 in the same ratio (95:5 wt/wt) were tested in order to assess the degree of viscosity of the  
139 binder. The coal was pre-heated to reduce its volatile matter content, which causes  
140 scattering of the data, and to make clear the influence of the binder on the complex  
141 viscosity of the blend. The pre-heating of the coal was conducted following fast heating  
142 at 40 °C min<sup>-1</sup> from room temperature to 520°C. In this process the coal temperature was  
143 monitored using a thermocouple inside the furnace, the final temperature detected for the  
144 sample was 466 ± 2 °C. During the experiments, the biomass samples were heated from  
145 50 °C to 400 °C at 3 °C/min. The coking coal and the blends of coal with binders or  
146 biomass samples were heated from room temperature to 330 °C at around 85 °C/min and  
147 from 330 °C to 500 °C at 3 °C/min. The complex viscosity was calculated using Eq. (1),  
148 where G' is the storage or elastic modulus, G'' is the loss or viscous modulus and ω is the  
149 frequency.<sup>21</sup>

150

$$151 \quad \eta^*(\text{Pa.s}) = \frac{\sqrt{\{G'(\text{Pa})\}^2 + \{G''(\text{Pa})\}^2}}{\omega} \quad (1)$$

152

## 153 **2.6. Briquette preparation**

154 In order to optimize the composition of the briquettes, various trial runs were carried out  
155 in a briquetting press under a constant pressure of 100 bar. The briquettes were cylindrical  
156 in shape with 40 mm in diameter. The coal content in the briquette was always 70 wt%.  
157 The amount of biomass was kept at 15 wt% except when molasses were used as binder,  
158 in which case 20 wt% was the quantity employed. The briquettes also contained 15 wt%  
159 of binder except in the case of briquettes containing molasses, for which 10 wt% was  
160 used. Different amounts of binder were tested in the preparation of the briquettes but the  
161 total percentage of biomass plus binder was kept constant in order to compare the  
162 individual effects of these components. None of the liquid binders drained during  
163 pressing. The nomenclature used was, for example, T-Lg for a briquette prepared with  
164 coal, lignin and coal tar as binder and T/CTS-BIOC for a briquette prepared with coal,  
165 BIOC and a 1:1 wt/wt blend of coal tar and coal tar sludge.

166

## 167 **2.7. Gieseler fluidity of briquette mixtures**

168 The thermoplastic properties of the mixtures that made up the briquettes were measured  
169 by means of the Gieseler test (ASTM D2639-74).<sup>22-24</sup> The samples (5 g), with a particle  
170 size < 0.425 mm, were heated at a rate of 3 °C/min up to a final temperature of 550 °C,  
171 while constantly applying a torque to the stirrer inside the crucible containing the sample.  
172 The parameters derived from this test were: (i) softening temperature, Ts; (ii) temperature  
173 of maximum fluidity, Tf; (iii) resolidification temperature, Tr; (iv) plastic range, Tr-Ts;  
174 and (v) maximum fluidity, MF, expressed as dial divisions per minute (ddpm).

175

## 176 **3. Results and Discussion**

### 177 **3.1. Thermogravimetric analysis of raw materials**

178 The TGA curves corresponding to the mass loss and the derivative of the mass loss curves  
179 of the briquette components are shown in **Figure 1**. The plots are presented in wet basis. The  
180 vertical dash line in the plots represents the temperature of maximum fluidity or minimum  
181 viscosity of coal (435 °C), calculated as the average of Gieseler plastometry (440 °C) and  
182 rheometry (430 °C) results. The curves for the variation of mass loss of the biomass with  
183 temperature indicate that, at 435 °C, the highest char yield corresponds to Lg (55 wt%),  
184 followed by BIOC and SPT (43 wt% and 40 wt%, respectively) and by SP (21 wt%), which  
185 is in agreement with the carbon contents (**Table 1**). With regard to the binders, the highest  
186 coke yield at 435 °C corresponds to T (38 wt%), followed by CTS and Mol (28 wt% and 24  
187 wt%, respectively) and Par (0.2 wt%), with the latter almost volatilizing completely at 400  
188 °C. The maximum devolatilization rate occurs at around 450 °C in the coal, 330 °C in SP,  
189 SPT, BIOC and Lg, 300 °C in Par and 200 °C in Mol. T and CTS do not show a clear  
190 maximum in the devolatilization rate.

191

### 192 **3.2. Infrared spectroscopy of raw materials**

193 The chemical composition of the additives is important as it might influence coal fluidity.  
194 Tsubouchi et al.<sup>25</sup> reported that the Gieseler maximum fluidity (MF) values tend to decrease  
195 with the increase in the total amount of evolved oxygenated species during carbonization  
196 (mainly CO, CO<sub>2</sub> and H<sub>2</sub>O). These authors attributed the release of these species to the  
197 presence of carboxyl and acid anhydride groups. On the other hand, another study on the  
198 development of fluidity in biomass and coal blends<sup>18</sup> reported that the higher the carbonyl  
199 groups and the lower the aromatic carbon in biomass, the lower the detrimental effect on



200 coal fluidity. Aromaticity has also been reported to be an important factor in the  
201 enhancement of fluidity. Polycondensed aromatics can provide a pathway for the transfer  
202 of hydrogen to radical sites in bituminous coals, and thereby, act as intermediates in the  
203 transformation of coal to coke.<sup>26,27</sup> Sharma et al.<sup>28</sup> also emphasized the importance of the  
204 C/H atomic ratio of the binder because it has a decisive effect on the strength of the briquettes  
205 under differing thermo-chemical conditions of curing and carbonization. These authors  
206 indicated that binders with C/H ratios above 1 are preferable for the production of briquettes.

207

208 **Table 1** shows that Mol has the highest oxygen content (55.9 wt%), followed by SP (44.7  
209 wt%). As expected, the heat-treated sample SPT has lower amounts of oxygen than SP (35.5  
210 wt% cf. 44.7 wt%). The oxygen content in Lg (26.3 wt%) is comparable to that in BIOC  
211 (25.5 wt%). T and CTS have lower oxygen contents than those in the biomass samples (3.0  
212 wt% and 8.2 wt%, respectively). The oxygen content in paraffin is almost insignificant (0.3  
213 wt%). Regarding the C/H ratio (**Table 1**), both bituminous binders have a ratio between  
214 1.3–1.6, which is desirable (i.e. > 1). In the case of the other two binders the ratios are lower  
215 (< 0.5), being the lowest C/H ratio that of Mol (0.3).

216

217 **Figures 2 and 3** display the FTIR spectra of the biomass samples and the binders,  
218 respectively. The FTIR spectrum of the bituminous coal is also presented in **Figure 3** for  
219 comparison purposes. Several bands can be observed in the ATR infrared spectra of the  
220 biomass samples (**Figure 2**). The broad and intense peak around  $3300\text{ cm}^{-1}$  is attributed to  
221 the stretching of the O–H group due to inter and intramolecular hydrogen bonding of  
222 cellulosic compounds, such as alcohols and phenols.<sup>29</sup> The range between  $2990\text{ cm}^{-1}$  and  
223  $2765\text{ cm}^{-1}$  is assigned to the aliphatic stretching of C–H, the  $1770\text{--}1650\text{ cm}^{-1}$  range

224 originates from C=O bonds and the 1600 cm<sup>-1</sup> band is assigned to C=C stretching vibrations  
225 of the aromatic rings.<sup>12</sup> The absorption bands at around 1230 cm<sup>-1</sup> and 1060 cm<sup>-1</sup> correspond  
226 to C–O stretching, and at 1027 cm<sup>-1</sup> there is a strong C–O bond attributed to the ether group  
227 of cellulose.<sup>29,30</sup> The spectra for SP and SPT are fairly similar. Mol, BIOc and Lg possess  
228 higher concentrations of C=O groups (1770–1650 cm<sup>-1</sup>) and C=C bonds of aromatic rings  
229 (1600 cm<sup>-1</sup>) than SP and SPT. Mol presents the highest content of O–H groups (3300 cm<sup>-1</sup>).

230

231 **Figure 3** shows the ATR infrared spectra of the low rank coal, paraffin, coal tar and coal tar  
232 sludge. The aromatic and aliphatic C–H stretching modes appear at 3100–2990 cm<sup>-1</sup> and  
233 2990–2765 cm<sup>-1</sup>, respectively.<sup>12</sup> The C=O band appears between 1800–1633 cm<sup>-1</sup> and C=C  
234 stretching modes appear between 1633–1538 cm<sup>-1</sup>.<sup>12</sup> Flexions in methylene and methyl  
235 groups are observed at 1450 cm<sup>-1</sup> and 1375 cm<sup>-1</sup>, respectively. The 900–700 cm<sup>-1</sup> range  
236 corresponds to the out-of-plane aromatic C–H vibration modes and reveals differences in  
237 the substitution patterns of the aromatic structures.<sup>31</sup> The strong peak in the spectrum of  
238 paraffin at 720 cm<sup>-1</sup> has been ascribed to the in-plane rocking vibration of the –CH<sub>2</sub> group.<sup>32</sup>  
239 The spectra of T and CTS are fairly similar and very different to those of Par and the  
240 bituminous coal. Par is mainly constituted by aliphatic C–H groups whereas T and CTS  
241 mainly contain aromatic C–H groups.

242

243 **Table 3** presents the semi-quantitative indices previously defined in **Table 2**. The A<sub>OH</sub>/A<sub>C=O</sub>  
244 index, which gives information about the distribution of oxygen functionalities, decreases in  
245 the following order for the biomass samples: SP (23.82) >> Mol (13.40) >> BIOc (8.37) ≈  
246 SPT (7.45) = Lg (7.45). Most of the oxygen species present in SP are O–H groups. Mol  
247 shows a large amount of both O–H and C=O groups, which is in agreement with the results  
248 from other authors.<sup>30</sup> The heat-treated biomass samples SPT and BIOc have lower

249 proportions of the O–H bond as indicated by the low  $A_{\text{OH}}/A_{\text{C=O}}$  index values ( $< 9$ ). This  
250 index was not calculated for the coal, due to the interference of mineral matter, or for the  
251 bituminous binders and Par, as the band due to O–H is not apparent in the spectra (Figure  
252 3).

253

254 The  $A_{\text{C=C}}/A_{\text{al}}$  index was calculated to determine semi-quantitatively the degree of  
255 aromaticity of the samples. Mol and BIOc are the most aromatic biomass samples (0.43 and  
256 0.46), whereas SP has the lowest value (0.33). The highest aromaticity corresponds to T  
257 (0.74) and CTS (0.63). Coal has a lower  $A_{\text{C=C}}/A_{\text{al}}$  ratio (0.35) than some biomass samples  
258 due to the large amount of aliphatic hydrogen in the coal used due to its rank.<sup>33</sup> This index  
259 was not calculated for paraffin because it does not show a band at  $1600\text{ cm}^{-1}$ .

260

### 261 3.3. High-temperature $^1\text{H}$ NMR of raw materials

#### 262 3.3.1. Changes in the concentration of fluid H

263 Figure 4 shows the development of fluid H as a function of temperature for the raw  
264 materials. Mol, T and CTS have not been included in the graph because they remain liquid  
265 (i.e. 100% fluid H) throughout the test. The fluid H profiles of BIOc, SP and SPT are very  
266 similar and show two maxima: one at around  $100\text{ }^\circ\text{C}$ , mainly due to the evaporation of water,  
267 and the other one at around  $300\text{ }^\circ\text{C}$ . The maximum percentages of fluid H and the  
268 temperatures of maximum fluid H for BIOc, SP and SPT are similar to those of miscanthus  
269 (i.e. 25% fluid H and  $330\text{ }^\circ\text{C}$ ).<sup>20</sup> Lignin develops fluidity between  $200\text{--}400\text{ }^\circ\text{C}$  and reaches  
270 a maximum of 80% fluid H at around  $300\text{ }^\circ\text{C}$ . The fluid phase development of coal takes  
271 place at higher temperatures ( $375\text{--}500\text{ }^\circ\text{C}$ ), reaching a maximum of 90% fluid H at  $460\text{ }^\circ\text{C}$ ,  
272 in agreement with results from the literature.<sup>34</sup> Paraffin becomes completely fluid at  $75\text{ }^\circ\text{C}$ ,  
273 and remains fluid until it completely devolatilizes at around  $400\text{ }^\circ\text{C}$ .

274

### 275 **3.3.2. Changes in the mobility of the fluid H**

276 **Figures 5a and 5b** show the changes in the spin-spin relaxation time (T2L), or mobility of  
277 the fluid H, as a function of temperature for the raw materials. Similarly to the development  
278 of fluid H, SP, SPT and BIOC display similar mobility profiles (**Figure 5a**). These biomass  
279 samples have three maxima: the first one at around 75 °C; the second one depends on the  
280 biomass (SPT at 150 °C and SP and BIOC at 200 °C); and the third one at 325 °C. Lg only  
281 has two maxima, one at around 75 °C and the other at around 300 °C. These changes in  
282 mobility seem to be related to the evaporation of water (75 °C) and the decomposition of  
283 hemicellulose, cellulose and lignin constituents. A previous study<sup>35</sup> has shown that the T2L  
284 of cellulose reaches a maximum of 300  $\mu\text{s}$  at 150 °C. The same authors found that xylan,  
285 which represents 90% of the hemicellulose, reaches the maximum T2L of 450  $\mu\text{s}$  at a higher  
286 temperature than cellulose (around 175 °C cf. 150 °C) and that Lg maintains a T2L value of  
287 around 200  $\mu\text{s}$  between 250–350 °C. In light of this, the maximum T2L at 150 °C of SPT  
288 could be related to the mobility of cellulose, whereas the wide T2L peak of SP at 200 °C  
289 could be due to the combination of cellulose and hemicellulose mobilities. The changes in  
290 mobility of the fluid H in the case of miscanthus<sup>35</sup> are similar to the results for SP reported  
291 in the present research work. The maximum T2L of 200  $\mu\text{s}$  at around 300 °C could be  
292 associated with the aromatic structures in biomass (i.e. lignin).

293

294 The development of T2L for the low rank bituminous coal takes place between 400–500 °C,  
295 reaching a maximum of 150  $\mu\text{s}$  at around 450 °C (**Figure 5b**). Among the binders, molasses  
296 develops the lowest maximum T2L (ca. 115  $\mu\text{s}$ ). Paraffin exhibits a maximum T2L of 276  
297  $\mu\text{s}$  at 75 °C, but also reaches mobilities of 220  $\mu\text{s}$  between 300–400 °C. T presents a  
298 maximum T2L of 286  $\mu\text{s}$  at 100 °C. The T2L profiles of T and CTS are very similar from

299 200 °C onwards, remaining constant at around 160  $\mu$ s and 150  $\mu$ s, respectively. Out of all  
300 these additives, only coal tar and coal tar sludge develop mobility of fluid H that is equal to  
301 or higher than the mobility of fluid H in the coal during its plastic stage (80–150  $\mu$ s).

302

### 303 **3.4. High-Temperature Rheometry**

304 **Figure 6a** shows the variation in complex viscosity as a function of temperature for the  
305 biomass samples and the coal. SP and SPT display a small decrease in complex viscosity,  
306 which reaches a minimum of  $1 \times 10^6$  Pa.s at around 343 °C. The development of viscosity  
307 for sawdust and miscanthus follows a similar trend,<sup>18</sup> in line with the similarities previously  
308 mentioned for the fluid phase and mobility developments of these samples. The complex  
309 viscosity of lignin is very similar to the elastic and viscous moduli described in the  
310 literature.<sup>20</sup> Lignin shows a lower minimum in complex viscosity ( $1 \times 10^4$  Pa.s) than the other  
311 biomass samples. In contrast, BIOC did not experience any decrease in viscosity during the  
312 thermal treatment, although it showed fluid H and T2L development. This finding suggests  
313 that the fluid H in BIOC is not able to alter the viscoelastic properties of the bulk material.  
314 Coal reached a minimum of  $6 \times 10^3$  Pa.s at 427 °C, in agreement with the results found for  
315 other coals with high volatile matter.<sup>36</sup>

316

317 The rheometry analyses of the high volatile coal and its blends with the additives (5 wt%)  
318 are shown in the Supplementary Material section (**Figure SM1**). Only a few noteworthy  
319 changes were observed. Biomass samples cause a slight shift of the softening and minimum  
320 viscosity temperatures of the coal to higher temperatures and the resolidification of the blend  
321 containing SP is the slowest in the series.

322

323 The coal was pre-heated to reduce data scattering and to clearly elucidate the influence of  
324 the binders on the viscosity of the blends. **Figure 6b** shows the complex viscosity analysis  
325 of blends made up of 5 wt% binder and 95 wt% pre-heated coal (C466). Under these  
326 conditions, coal tar and coal tar sludge cause a remarkable decrease in the softening  
327 temperature range and the minimum viscosity temperature (413 °C vs. 423 °C), in agreement  
328 with data from the literature.<sup>37</sup> Par also causes a reduction in the softening temperature range  
329 (360–385 °C) but additional heating does not entail any significant change compared to that  
330 of the pre-heated coal up to the temperature of minimum viscosity (423 °C). Melendi et al.<sup>38</sup>  
331 showed that polyolefins and hydrocarbon oil are weaker modifiers of coal's rheological  
332 properties, which is in agreement with our results for Par. Finally, the softening and  
333 minimum viscosity temperatures of the blend with molasses rise (435 °C vs. 423 °C). A  
334 previous research work focusing on the effect of biomass (i.e. pine wood, sugar beet,  
335 miscanthus) on fluidity development in coking blends did not show this effect for blends  
336 with a coal of moderate VM content (25.2 wt% daf) and a Gieseler fluidity of 817 ddpm.<sup>18</sup>  
337 However, similar results were obtained by these authors through rheometry analysis of a  
338 high volatile bituminous coal (31.9 wt% db) mixed with miscanthus. This effect has also  
339 been reported during the analyses of blends of a bituminous coal (VM, 25.2 wt% db) with  
340 charcoal, wood and other additives.<sup>34</sup> The addition of coal tar sludge or paraffin causes a  
341 decrease in the resolidification temperature. On the contrary, the resolidification stage takes  
342 place at a higher temperature when molasses are added. The values of the minimum complex  
343 viscosity for C466 and its blends is about  $1.5 \times 10^4$  Pa.s, except with molasses, which is less  
344 viscous ( $3 \times 10^4$  Pa.s).

345

### 346 **3.5. Thermoplastic properties of ternary blends constituting the briquettes**

347 The results of the Gieseler fluidity tests in this work are shown in **Table 4** and **Figure 7**. The  
348 high volatile, high fluidity bituminous coal (26000 ddpm) was chosen in this work to prepare  
349 the briquettes taking into consideration the deleterious effect of biomass on the plastic  
350 properties of coal. It is envisaged that the resultant briquettes should be capable of  
351 developing suitable levels of fluidity.<sup>8,18,39</sup> The importance of this feature cannot be  
352 underestimated since the lack of fluidity can affect the integration of briquettes into the coke  
353 matrix, which would increase the possibility of fissures, affecting the quality of the final  
354 coke product.<sup>40</sup> The components of a coal blend soften independently and, as a consequence,  
355 the plastic range of a blend may be wider than that of the base coal. It is also necessary to  
356 bear in mind that the properties of the softened mass may be influenced by interactions  
357 between the softened and inert components of the blend.<sup>37</sup> In the present research work, the  
358 blends used were complex and made up of products that, when individually added to the  
359 coal, can have opposite effects. In summary, biomass has been found to decrease fluidity  
360 and move the plastic stage to higher temperatures, T and CTS produce a decrease in the  
361 softening range of the coal, and Par has very little effect on coal fluidity.

362

363 The softening, maximum fluidity and resolidification temperatures of the ternary blends  
364 are displayed in **Table 4**. No systematic trend can be observed for the softening  
365 temperature of the blends containing T and CTS compared with blends containing Par.  
366 On the other hand, blends with Mol show the highest softening temperatures. However,  
367 examination of the temperature of maximum fluidity (Tf) and the Gieseler curves in  
368 **Figure 7** shows lower Tf values for blends with aromatic binders than with Par. In fact,  
369 the maximum fluidity temperatures of blends containing Par and Mol are very close to  
370 each other. Mol also produces resolidification at the lowest temperatures. As a result, their  
371 blends have the narrowest plastic range, which is defined by the difference between the

372 resolidification and softening temperatures (Tr-Ts). This finding is in agreement with the  
373 rheometry results (Figure 6b). The Gieseler plastometer results in Table 4 also indicate  
374 that the Tr of coal is always equal to or higher than the Tr of the blends.

375

376 For the same binder, the following order of increasing deleterious effect of the biomass  
377 upon the thermoplastic properties of the coal has been established:

378

379 
$$SP < BIOC < SPT < Lg$$

380

381 Although there are some exceptions, SP and BIOC develop similar MF with T/CTS as  
382 binder, as in the case of SPT and BIOC with blends containing Par. A previous research  
383 work established that torrefied sawdust produced a slightly greater reduction in Gieseler  
384 maximum fluidity than sawdust that had not been heat-treated.<sup>8</sup> It would appear that this  
385 result is related to the char yield of the biomass, as shown in Figure 8a. BIOC is an  
386 exception to this correlation because it produces only a small deleterious effect in blends  
387 with bituminous binders. For this reason, these blends have not been taken into account  
388 when calculating the correlation coefficients.

389 There is some debate as to the influence of the oxygen content on fluidity. Previous  
390 studies by Tsubouchi et al.<sup>25</sup> have shown that oxygen species can have a deleterious  
391 effect. Whereas, other authors have shown using <sup>13</sup>C NMR that, the aromatic carbon in the  
392 biomass could have a detrimental effect and/or the carboxyl groups from hemicellulose  
393 could have a beneficial effect on coal fluidity<sup>18</sup>. Our results show that an increase in oxygen  
394 species is accompanied by smaller loss in MF (Figure 8b). However, there is also an inverse  
395 linear relationship between the coke yield and the oxygen content of biomass ( $R^2 = 0.82$ ).  
396 The oxygen species are highly reactive compounds that reduce the char yield from biomass.



397 As a result, the contact area between the evolving char and the fluid material of coal  
398 decreases and the impairment in coal fluidity is reduced by reducing the amount of biomass  
399 char, which might act as a sink for the fluid entities evolving in the coal.

400 Although it might appear that oxygen content has a positive effect, if two biomass samples  
401 with a similar char yield are compared, such as BIOC and SPT that produce char yields of  
402 around 42%, the less deleterious effect is caused by the biomass with lower oxygen content  
403 (i.e. BIOC, with 25.5% cf. 35.5% of SPT, Table 1). These results prove that oxygen species  
404 in biomass have a negative effect on coal fluidity.

405 The results in **Figures 8a and 8b** for blends containing the same biomass sample indicate  
406 that the binders cause a greater increase in fluidity in the following order:

407

408 
$$T > T/CTS > Par > Mol$$

409

410 These results do not seem to be related to the coke or char yields of the binders. Mol and  
411 CTS yield similar amounts of solid residue at the temperature of maximum fluidity of the  
412 coal, but they have completely opposite effects on the fluidity of the coal. However, a  
413 relationship has been found between the effect of the binders on the coal plastic properties  
414 and their C/H atomic ratio (**Figure 9**). In the case of Lg, the factor discussed above does  
415 not appear to be very significant, as can be seen by the low value of the correlation  
416 coefficient ( $R^2 = 0.672$ ), which suggests that the effect of this biomass constituent is  
417 predominant over that of the binder.

418

419 These results also confirm that the greater the char yield of the biomass, the greater the  
420 reduction in blend fluidity. Furthermore, the effect is even more pronounced in the case  
421 of the binders that have a greater C/H atomic ratio, and consequently, a greater effect on

422 the plastic properties of the coal. A combination of physical and chemical effects explains  
423 these results. On the one hand, the inert additives that are blended with the softening coal  
424 possibly reduce fluidity by adsorbing the primary decomposition compounds responsible  
425 for the development of fluidity.<sup>41,42</sup> On the other hand, the binders with higher C/H values  
426 are able to supply aromatic compounds that serve as stabilizers of the radicals formed  
427 during coal decomposition, compensating for the deleterious effect of chars present in the  
428 reaction system. Polycondensed aromatics can provide a pathway for the transfer of  
429 hydrogen to radical sites in bituminous coals, and thereby, act as intermediates in the  
430 transformation of coal to coke.<sup>26,27</sup> For any particular biomass, the least deleterious effect  
431 is produced if an aromatic binder is used.

432

433 Therefore, the biomass samples studied in this work that are more suitable for the  
434 preparation of the briquettes, considering their effect on the thermoplastic properties of  
435 coal, are SP and BIOC. In the case of the binders, T and CTS are the binders that best  
436 compensate for the deleterious effect of biomass on coal fluidity.

437

#### 438 **4. Conclusions**

439 Four biomass samples and four binders have been blended with a low rank bituminous coal  
440 to determine their effect on the thermoplastic properties of the coal. The biomass samples  
441 comprised of pine sawdust (SP), torrefied pine sawdust (SPT), pine Kraft lignin (Lg) and a  
442 bio-coal derived from hydrothermally treated waste biomass obtained from pruning (BIOC).  
443 The binders included molasses (Mol), paraffin (Par), coal tar (T) and coal tar sludge (CTS).  
444 The analysis of blends composed of coal, biomass and binder using the Gieseler plastometer  
445 has shown that the binder's effects, as identified by rheometry analysis, are sometimes  
446 modified by interaction with biomass. For the same binder, the following order of

447 increasing deleterious effect of the biomass upon the maximum fluidity of the coal has  
448 been established: SP < BIOC < SPT < Lg. It can also be deduced that for the same biomass  
449 the order of increasing deleterious effect of the binder on the coal maximum fluidity is as  
450 follows: T < T/CTS < Par < Mol. The coke yields of the biomass samples together with the  
451 chemical composition of the binders help to explain the fluidity of the blends.

452

453 The oxygen species in biomass have a negative effect on coal fluidity, these species are  
454 associated to highly reactive compounds that reduce the char yield from biomass. As a result,  
455 the contact area between the char from biomass and the fluid material of coal decreases and  
456 the impairment in coal fluidity is reduced.

457

458 Coal tar, coal tar sludge, pine sawdust and BIOC appear to be the best briquette components.  
459 Nevertheless, paraffin can be considered as a good alternative to bituminous binders because  
460 it does not cause any significant impairment of the thermoplastic properties of coal and it is  
461 less polluting. Future work must address other important factors such as optimum  
462 concentrations of biomass and binder in the briquettes and the impact of coal rank and coal  
463 blend composition in order to preserve coke quality and safeguard coke oven operation.

464

#### 465 **Acknowledgements**

466 The research leading to these results has received funding from the European Union's  
467 Research Fund for Coal and Steel (RFCS) research programme under grant agreement  
468 No. [RFCS-CT-2014-00006].

469

470 **References**

- 471 (1) Alvarez, R.; Barriocanal, C.; Díez, M. A.; Cimadevilla, J. L. G.; Casal, M. D.;  
472 Canga, C. S. Recycling of Hazardous Waste Materials in the Coking Process.  
473 *Environ. Sci. Technol.* **2004**, *38* (5), 1611–1615.
- 474 (2) Díez, M. A.; Alvarez, R.; Melendi, S.; Barriocanal, C. Feedstock Recycling of  
475 Plastic Wastes/Oil Mixtures in Cokemaking. *Fuel* **2009**, *88* (10), 1937–1944.
- 476 (3) Duffy, J. J.; Mahoney, M. R.; Steel, K. M. Influence of Coal Thermoplastic  
477 Properties on Coking Pressure Generation: Part 2 – A Study of Binary Coal  
478 Blends and Specific Additives. *17th Int. Symp. Alcohol Fuels* **2010**, *89* (7), 1600–  
479 1615.
- 480 (4) Fernández, A. M.; Barriocanal, C.; Alvarez, R. The Effect of Additives on  
481 Coking Pressure and Coke Quality. *Fuel* **2012**, *95*, 642–647.
- 482 (5) Mochida, I.; Matsuoka, H.; Korai, Y.; Fujitsu, H.; Takeshita, K. Carbonization of  
483 Coals to Produce Anisotropic Cokes. 1. Modifying Activities of Some Additives  
484 in the Co-Carbonization of Low-Rank Coals. *Fuel* **1982**, *61* (7), 587–594.
- 485 (6) Świetlik, U.; Gryglewicz, G.; Machnikowska, H.; Machnikowski, J.; Barriocanal,  
486 C.; Alvarez, R.; Díez, M. A. Modification of Coking Behaviour of Coal Blends  
487 by Plasticizing Additives. *J. Anal. Appl. Pyrolysis* **1999**, *52* (1), 15–31.
- 488 (7) Montiano, M. G.; Díaz-Faes, E.; Barriocanal, C.; Alvarez, R. Influence of  
489 Biomass on Metallurgical Coke Quality. *Fuel* **2014**, *116*, 175–182.
- 490 (8) Montiano, M. G.; Barriocanal, C.; Alvarez, R. Effect of the Addition of Waste  
491 Sawdust on Thermoplastic Properties of a Coal. *Fuel* **2013**, *106* (4), 537–543.
- 492 (9) Norgate, T.; Haque, N.; Somerville, M.; Jahanshahi, S. Biomass as a Source of  
493 Renewable Carbon for Iron and Steelmaking. *ISIJ Int.* **2012**, *52* (8), 1472–1481.

- 494 (10) Montiano, M. G.; Díaz-Faes, E.; Barriocanal, C. Partial Briquetting vs Direct  
495 Addition of Biomass in Coking Blends. *Fuel* **2014**, *137*, 313–320.
- 496 (11) Montiano, M. G.; Fernández, A. M.; Díaz-Faes, E.; Barriocanal, C. Tar from  
497 Biomass/Coal-Containing Briquettes. Evaluation of PAHs. *Fuel* **2015**, *154*, 261–  
498 267.
- 499 (12) Florentino-Madiedo, L.; Díaz-Faes, E.; García, R.; Barriocanal, C. Influence of  
500 Binder Type on Greenhouse Gases and PAHs from the Pyrolysis of Biomass  
501 Briquettes. *Fuel Process. Technol.* **2018**, *171*, 330–338.
- 502 (13) Castro-Díaz, M.; Zhao, H.; Kokonya, S.; Dufour, A.; Snape, C. E. The Effect of  
503 Biomass on Fluidity Development in Coking Blends Using High-Temperature  
504 SAOS Rheometry. *Energy Fuels* **2012**, *26* (3), 1767–1775.
- 505 (14) Menéndez, J. A.; Pis, J. J.; Alvarez, R.; Barriocanal, C.; Fuente, E.; Díez, M. A.  
506 Characterization of Petroleum Coke as an Additive in Metallurgical Cokemaking.  
507 Modification of Thermoplastic Properties of Coal. *Energy Fuels* **1996**, *10* (6),  
508 1262–1268.
- 509 (15) Mulligan, M. J.; Thomas, K. M. Some Aspects of the Role of Coal  
510 Thermoplasticity and Coke Structure in Coal Gasification: 3. The Effect of Rank,  
511 Pitch and Sodium Carbonate on Brabender Plastometry Parameters. *Fuel* **1987**,  
512 *66* (9), 1289–1298.
- 513 (16) Lynch, L. J.; Sakurovs, R.; Barton, W. A. The Influence of Iron on Proton  
514 Nuclear Magnetic Resonance Measurements of Coals. *Fuel* **1986**, *65* (8), 1108–  
515 1111.
- 516 (17) Maroto-Valer, M. M.; Andrésen, J. M.; Snape, C. E. In-Situ <sup>1</sup>H NMR  
517 Investigation of Particle Size, Mild Oxidation, and Heating Regime Effects on

- 518 Plasticity Development during Coal Carbonization. *Energy Fuels* **1997**, *11* (1),  
519 236–244.
- 520 (18) Castro-Díaz, M.; Zhao, H.; Kokonya, S.; Dufour, A.; Snape, C. E. The Effect of  
521 Biomass on Fluidity Development in Coking Blends Using High-Temperature  
522 SAOS Rheometry. *Energy Fuels* **2012**, *26* (3), 1767–1775.
- 523 (19) Barriocanal, C.; Díez, M.; Alvarez, R.; Casal, M.; Canga, C. On the Relationship  
524 between Coal Plasticity and Thermogravimetric Analysis. *J. Anal. Appl.*  
525 *Pyrolysis* **2003**, *67* (1), 23–40.
- 526 (20) Dufour, A.; Castro-Díaz, M.; Marchal, P.; Brosse, N.; Olcese, R.; Bouroukba, M.;  
527 Snape, C. In Situ Analysis of Biomass Pyrolysis by High Temperature Rheology  
528 in Relations with <sup>1</sup>H NMR. *Energy Fuels* **2012**, *26* (10), 6432–6441.
- 529 (21) Steel, K. M.; Castro-Díaz, M.; Patrick, J. W.; Snape, C. E. Use of Rheometry and  
530 <sup>1</sup>H NMR Spectroscopy for Understanding the Mechanisms behind the  
531 Generation of Coking Pressure. *Energy Fuels* **2004**, *18* (5), 1250–1256.
- 532 (22) Melendi, S.; Díez, M. A.; Alvarez, R.; Barriocanal, C. Plastic Wastes, Lube Oils  
533 and Carbochemical Products as Secondary Feedstocks for Blast-Furnace Coke  
534 Production. *Fuel Process. Technol.* **2011**, *92* (3), 471–478.
- 535 (23) Fernández, A. M.; Barriocanal, C.; Díez, M. A.; Alvarez, R. Influence of  
536 Additives of Various Origins on Thermoplastic Properties of Coal. *Fuel* **2009**, *88*  
537 (12), 2365–2372.
- 538 (24) Barriocanal, C.; Patrick, J. W.; Walker, A. The Laboratory Identification of  
539 Dangerously Coking Coals. *Fuel* **1998**, *77* (8), 881–884.
- 540 (25) Tsubouchi, N.; Mochizuki, Y.; Naganuma, R.; Kamiya, K.; Nishio, M.; Ono, Y.;  
541 Uebo, K. Influence of Inherent Oxygen Species on the Fluidity of Coal during  
542 Carbonization. *Energy Fuels* **2016**, *30* (3), 2095–2101.

- 543 (26) Grint, A.; Mehani, S.; Trehwella, M.; Crook, M. J. Role and Composition of the  
544 Mobile Phase in Coal. *Fuel* **1985**, *64* (10), 1355–1361.
- 545 (27) Díez, M. A.; Domínguez, A.; Barriocanal, C.; Alvarez, R.; Blanco, C. G.; Canga,  
546 C. S. Hydrogen Donor and Acceptor Abilities of Pitches from Coal and  
547 Petroleum Evaluated by Gas Chromatography. *J. Chromatogr. A* **1999**, *830* (1),  
548 155–164.
- 549 (28) Sharma, A. K.; Das, B. P.; Tripathi, P. S. M. Influence of Properties of  
550 Bituminous Binders on the Strength of Formed Coke. *Fuel Process. Technol.*  
551 **2002**, *75* (3), 201–214.
- 552 (29) Kaya, M. Evaluation of a Novel Woody Waste Obtained from Tea Tree Sawdust  
553 as an Adsorbent for Dye Removal. *Wood Sci. Technol.* **2018**, *52* (1), 245–260.
- 554 (30) El Darra, N.; Rajha, H. N.; Saleh, F.; Al-Oweini, R.; Maroun, R. G.; Louka, N.  
555 Food Fraud Detection in Commercial Pomegranate Molasses Syrups by UV–VIS  
556 Spectroscopy, ATR-FTIR Spectroscopy and HPLC Methods. *Food Control* **2017**,  
557 *78*, 132–137.
- 558 (31) Fernández, A. M.; Barriocanal, C.; Díez, M. A.; Alvarez, R. Evaluation of  
559 Bituminous Wastes as Coal Fluidity Enhancers. *Fuel* **2012**, *101*, 45–52.
- 560 (32) Chai, Y.; Zhao, T.; Gao, X.; Zhang, J. Low Cracking Ratio of Paraffin  
561 Microcapsules Shelled by Hydroxyl Terminated Polydimethylsiloxane Modified  
562 Melamine-Formaldehyde Resin. *Colloids Surf. Physicochem. Eng. Asp.* **2018**,  
563 *538*, 86–93.
- 564 (33) Casal, M. D.; Canga, C. S.; Díez, M. A.; Alvarez, R.; Barriocanal, C. Low-  
565 Temperature Pyrolysis of Coals with Different Coking Pressure Characteristics.  
566 *J. Anal. Appl. Pyrolysis* **2005**, *74* (1-2), 96–103.

- 567 (34) Castro Díaz, M.; Steel, K. M.; Drage, T. C.; Patrick, J. W.; Snape, C. E.  
568 Determination of the Effect of Different Additives in Coking Blends Using a  
569 Combination of in Situ High-Temperature <sup>1</sup>H NMR and Rheometry. *Energy*  
570 *Fuels* **2005**, *19* (6), 2423–2431.
- 571 (35) Dufour, A.; Castro-Díaz, M.; Brosse, N.; Bouroukba, M.; Snape, C. The Origin of  
572 Molecular Mobility during Biomass Pyrolysis as Revealed by in Situ <sup>1</sup>H NMR  
573 Spectroscopy. *ChemSusChem* **2012**, *5* (7), 1258–1265.
- 574 (36) Castro Díaz, M.; Duffy, J. J.; Snape, C. E.; Steel, K. M. Use of High-  
575 Temperature, High-Torque Rheometry to Study the Viscoelastic Properties of  
576 Coal during Carbonization. *J. Rheol.* **2007**, *51* (5), 895–913.
- 577 (37) Elliott, M. A. *Chemistry of Coal Utilization. Second Supplementary Volume*; John  
578 Wiley and Sons: Toronto, 1981; Vol. 6.
- 579 (38) Melendi-Espina, S.; Díez, M. A.; Alvarez, R.; Castro Díaz, M.; Steel, K.; Snape,  
580 C. Rheological Behaviour of Coal Modified by Waste Plastics and Lubricating-  
581 Oils; *Proceedings of the International Conference on Coal Science and*  
582 *Technology*, The University of Nottingham, August 28<sup>th</sup> - 31<sup>th</sup>, 2007; p. 2P45.
- 583 (39) Montiano, M. G.; Díaz-Faes, E.; Barriocanal, C. Effect of Briquette Composition  
584 and Size on the Quality of the Resulting Coke. *Fuel Process. Technol.* **2016**, *148*,  
585 155–162.
- 586 (40) Barriocanal, C.; Hanson, S.; Patrick, J. W.; Walker, A. The Characterization of  
587 Interfaces between Textural Components in Metallurgical Cokes. *Fuel* **1994**, *73*  
588 (12), 1842–1847.
- 589 (41) Sakurovs, R. Some Factors Controlling the Thermoplastic Behaviour of Coals.  
590 *Fuel* **2000**, *79* (3), 379–389.



591 (42) Fernández, A. M.; Barriocanal, C.; Díez, M. A.; Alvarez, R. Importance of the  
592 Textural Characteristics of Inert Additives in the Reduction of Coal  
593 Thermoplastic Properties. *Fuel* **2010**, *89* (11), 3388–3392.  
594

595

596 Table 1. Proximate and ultimate analysis of the briquette components.

	Coal	SP	SPT	BIOC	Lg	Mol	T	CTS	Par
Ash (wt% db) <sup>a</sup>	7.3	0.2	0.4	6.1	2.5	2.8 <sup>c</sup>	0.4 <sup>c</sup>	1.7 <sup>c</sup>	0.1 <sup>c</sup>
VM (wt% db) <sup>a,b</sup>	31.5	84.3	71.1	68.0	64.0	94.4 <sup>c</sup>	65.9 <sup>c</sup>	71.1 <sup>c</sup>	99.6 <sup>c</sup>
C (wt% db) <sup>a</sup>	81.2	50.9	59.8	59.8	64.7	26.5	90.3	84.2	85.1
H (wt% db) <sup>a</sup>	5.0	6.2	5.7	6.0	5.7	8.0	4.7	5.3	14.5
N (wt% db) <sup>a</sup>	1.6	0.3	0.3	1.2	0.9	1.7	0.8	1.3	0.2
S (wt% db) <sup>a</sup>	1.03	< 0.05	<0.05	0.15	1.52	0.18	0.40	0.60	<0.05
O (wt% db) <sup>a</sup>	4.8	44.7	35.5	25.5	26.3	55.9	3.0	8.2	0.3
C/H <sup>d</sup>	1.35	0.68	0.87	0.83	0.95	0.28	1.60	1.32	0.49

597

598 a: dry basis; b: volatile matter; c: determined in a thermobalance; d: atomic ratio

599 Table 2. Definition of the semi-quantitative indices derived from ATR infrared spectra.

Index	Description	Band region (cm <sup>-1</sup> )
Aromaticity ( $A_{C=C}/A_{al}$ )	$\nu$ C=C/ $\nu$ C-H aliphatic	A1600/A(3000–2800)
Oxygen distribution ( $A_{OH}/A_{C=O}$ )	$\nu$ OH/ $\nu$ C=O	A3000/A(1770–1650)

600  $\nu$ : stretching vibration;  $\sigma$ : bending vibration

601

602

Table 3. Values for the semi-quantitative indices of the briquette components.

	Coal	SP	SPT	BIOC	Lg	Mol	T	CTS	Par
$A_{OH}/A_{C=O}$	-	23.82	7.45	8.37	7.45	13.40	-	-	-
$A_{C=C}/A_{al}$	0.35	0.33	0.39	0.46	0.36	0.43	0.74	0.63	0.00

Table 4. Parameters derived from the Gieseler fluidity test of the coal and briquettes.

Sample	Ts (°C)	Tf (°C)	Tr (°C)	Tr-Ts (°C)	MF (ddpm)	MF loss (%)
Coal	382	439	484	102	26055	-
T-BIOC	386	434	479	93	2268	91.3
T/CTS-BIOC	384	433	481	97	2125	91.8
Mol-BIOC	404	443	466	62	69	99.7
Par-BIOC	384	444	479	95	395	98.5
T-Lg	342	433	475	133	389	98.5
T/CTS-Lg	342	436	475	133	340	98.7
Mol-Lg	-	-	-	-	-	100
Par-Lg	412	448	481	69	284	98.9
T-SP	387	432	483	96	3173	87.8
T/CTS-SP	392	434	482	90	2046	92.1
Mol-SP	403	442	475	72	242	99.1
Par-SP	378	441	486	108	922	96.5
T-SPT	394	438	481	87	962	96.3
T/CTS-SPT	389	440	476	87	999	96.2
Mol-SPT	416	446	467	51	11	99.9
Par-SPT	382	442	484	102	526	98.0

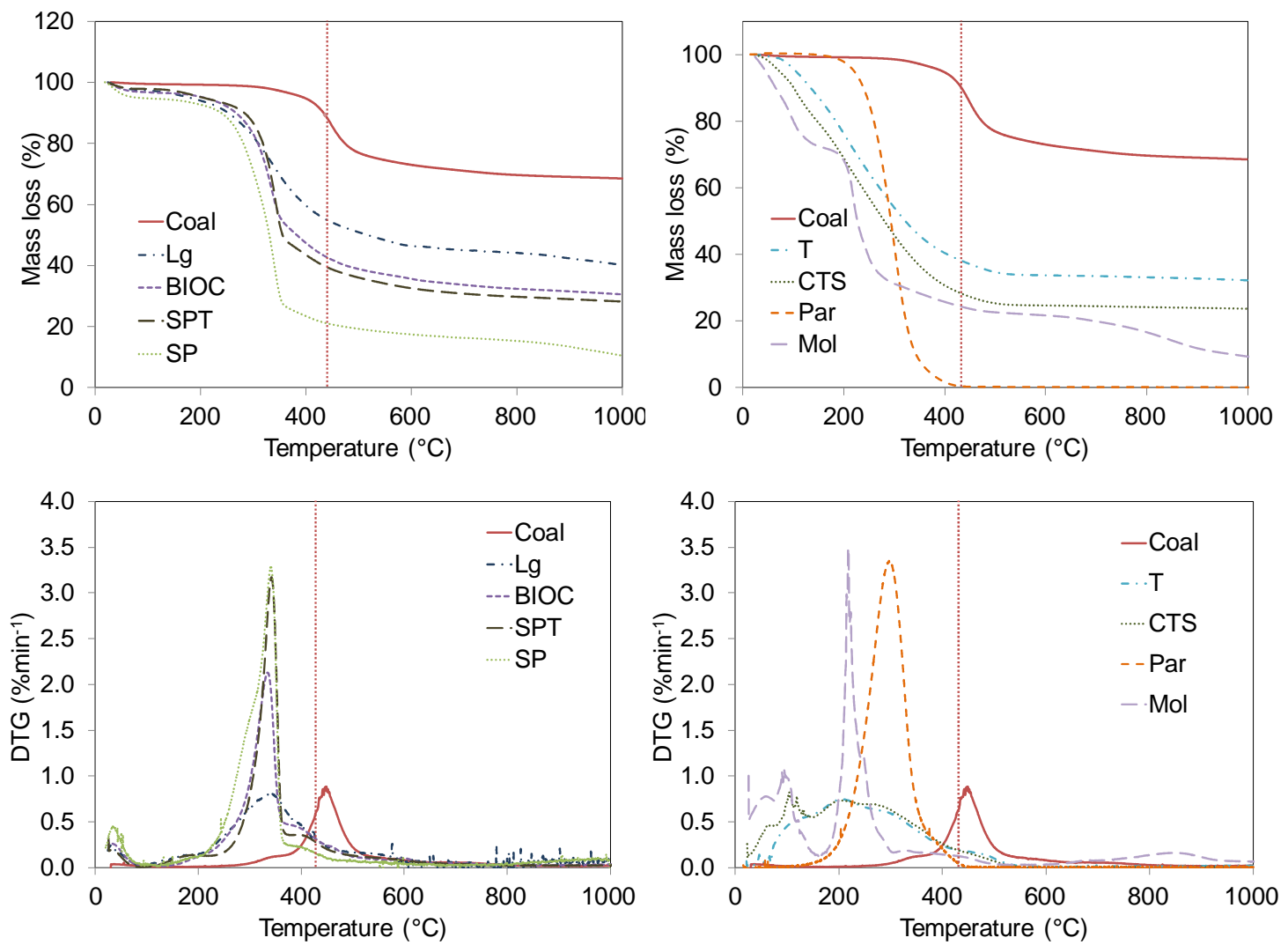


Figure 1. Mass loss of the raw materials as a function of temperature.

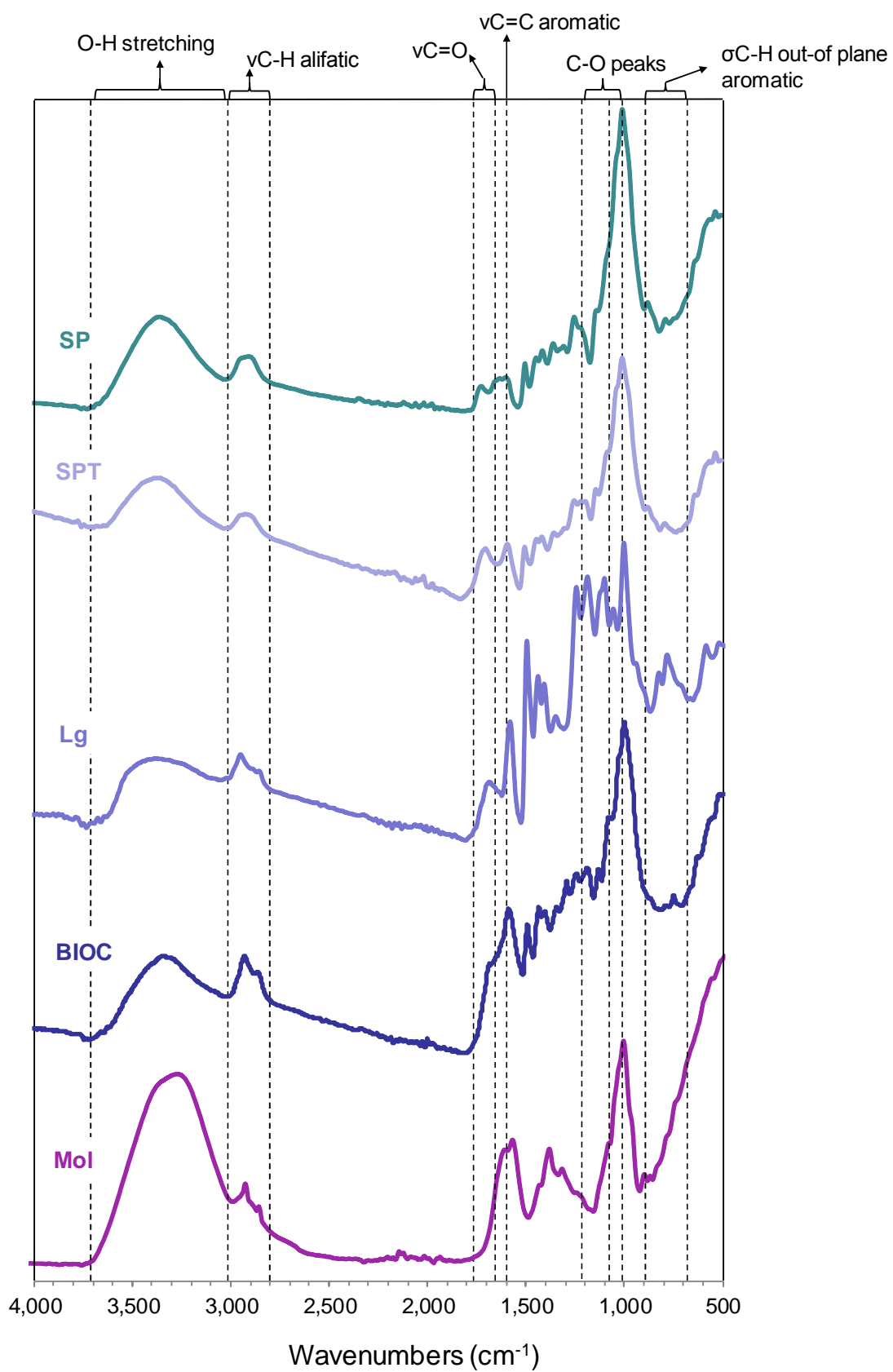


Figure 2. Infrared spectra of SP, SPT, Lg, BIOC and Mol.

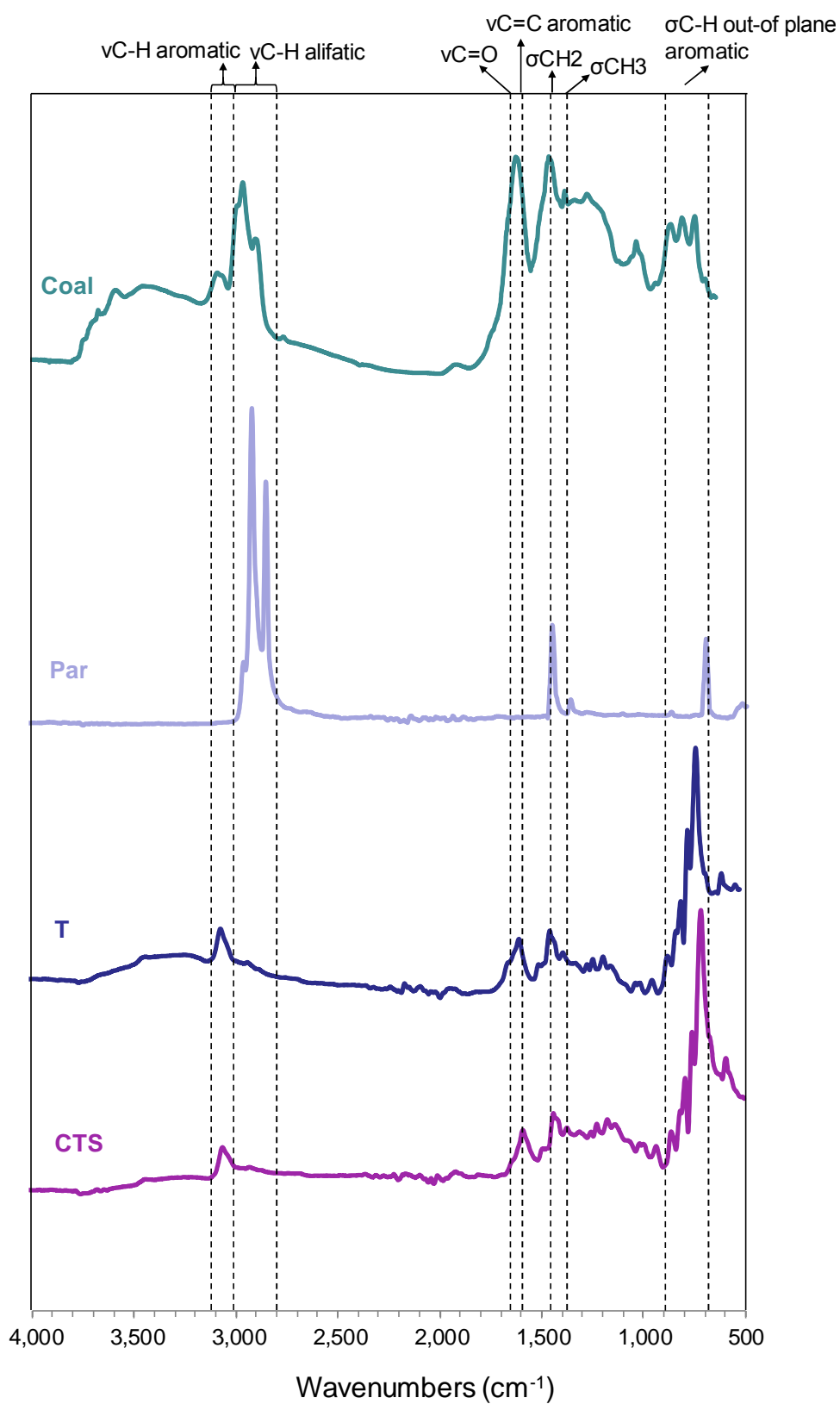


Figure 3. Infrared spectra of coal, Par, T and CTS.



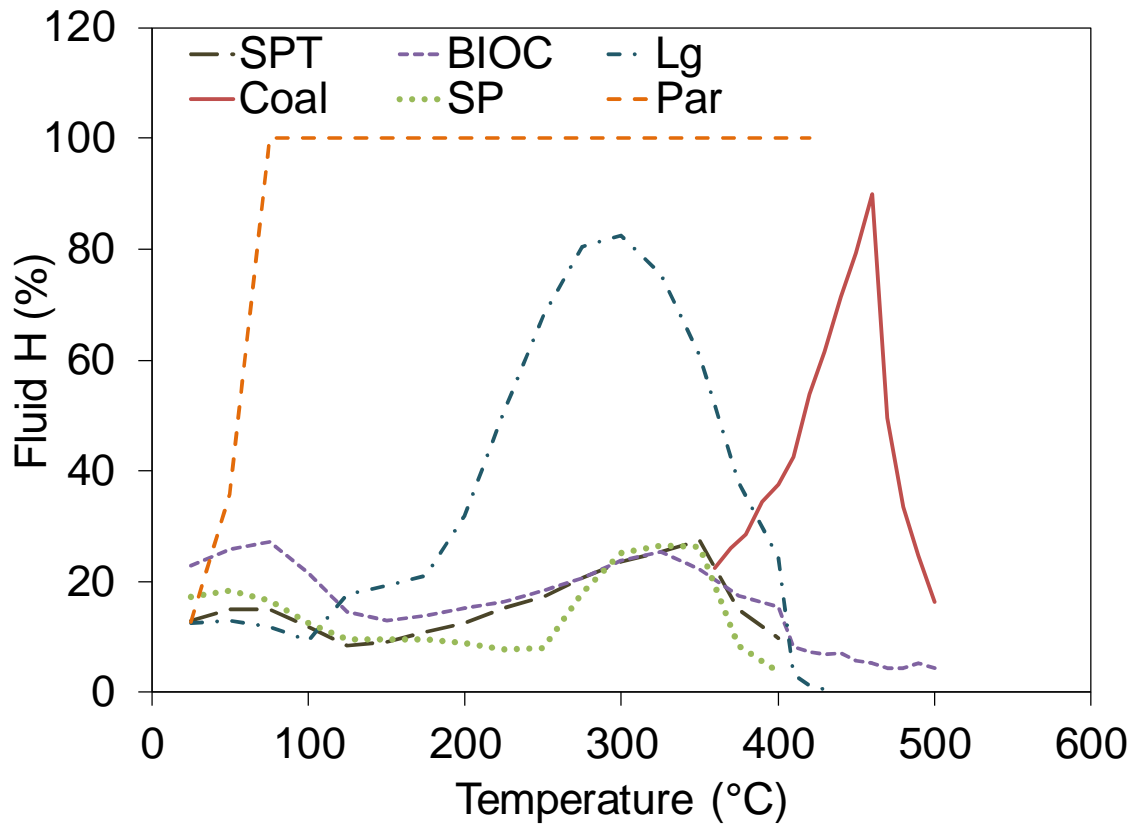


Figure 4. Fluid H development as a function of temperature.

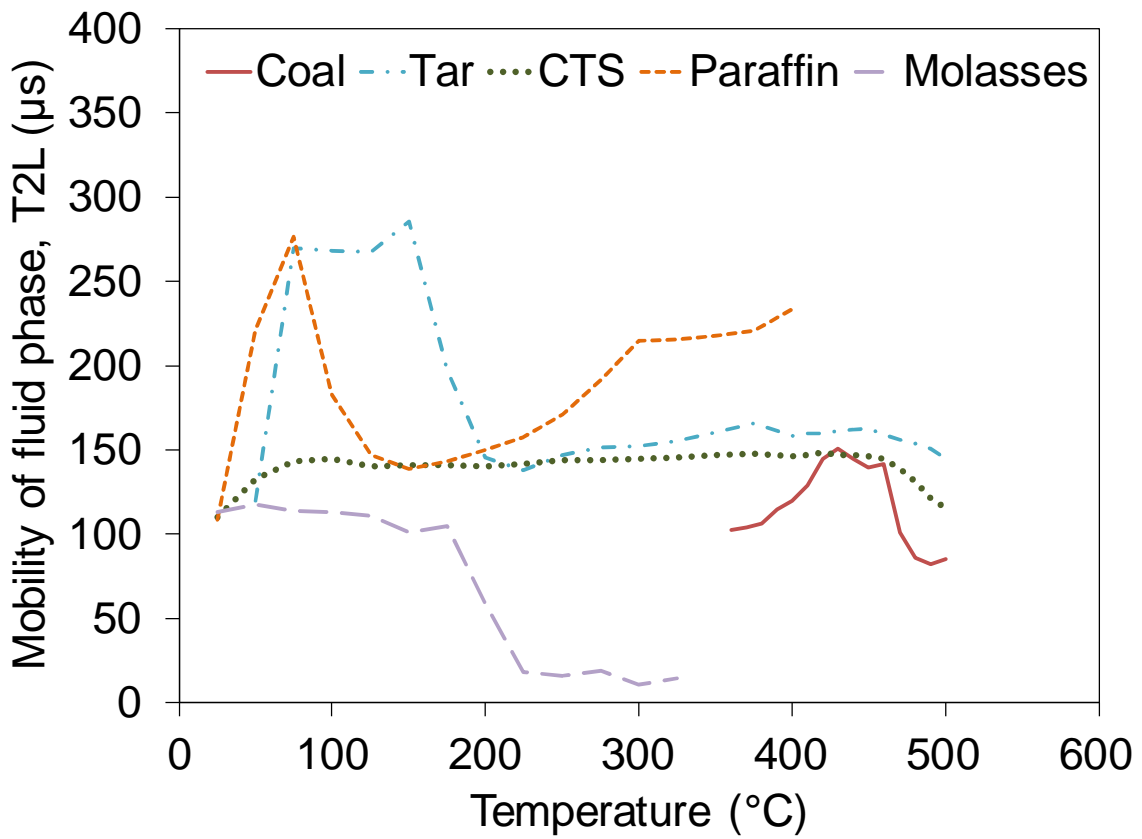
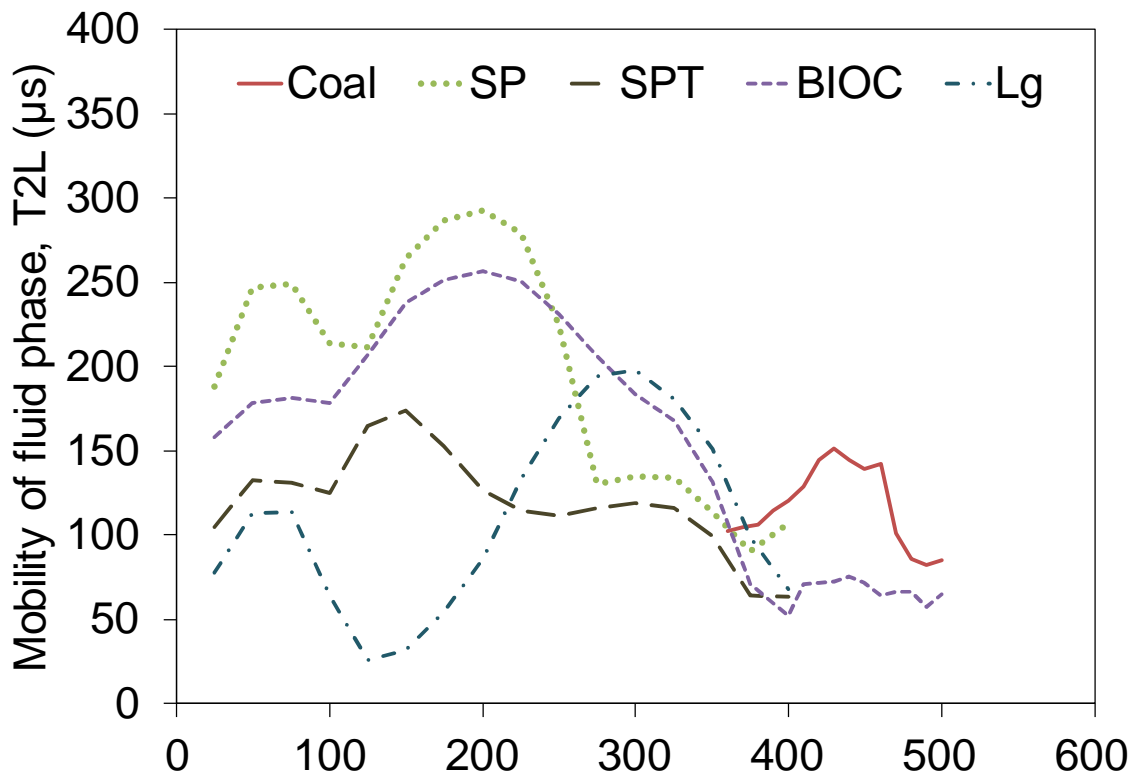


Figure 5. Changes in the mobility of fluid phase (T2L) as a function of temperature.

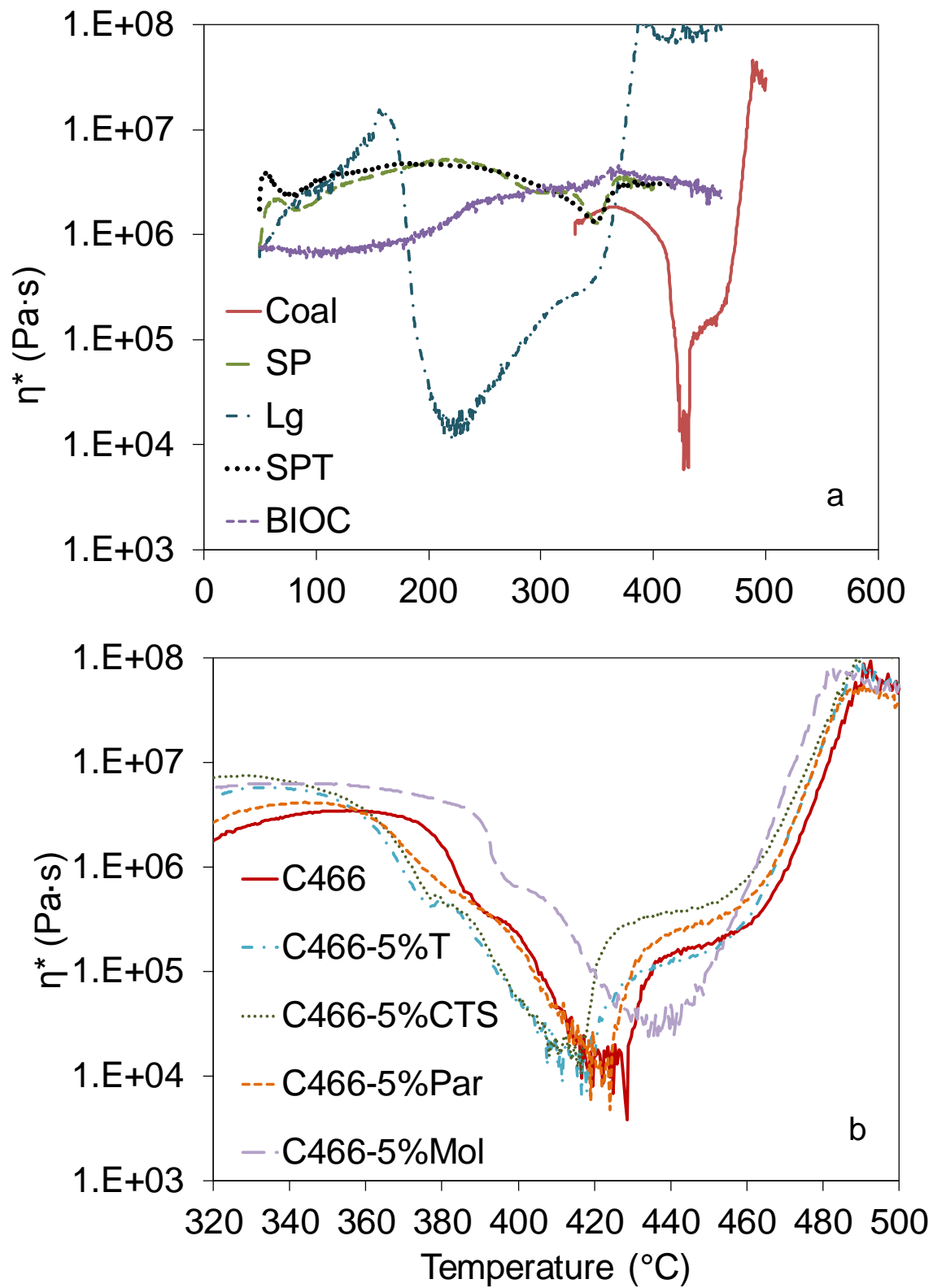


Figure 6. Complex viscosity as a function of temperature for a) coal and biomass samples and b) blends of coal pre-heated up to 466 °C with binders.

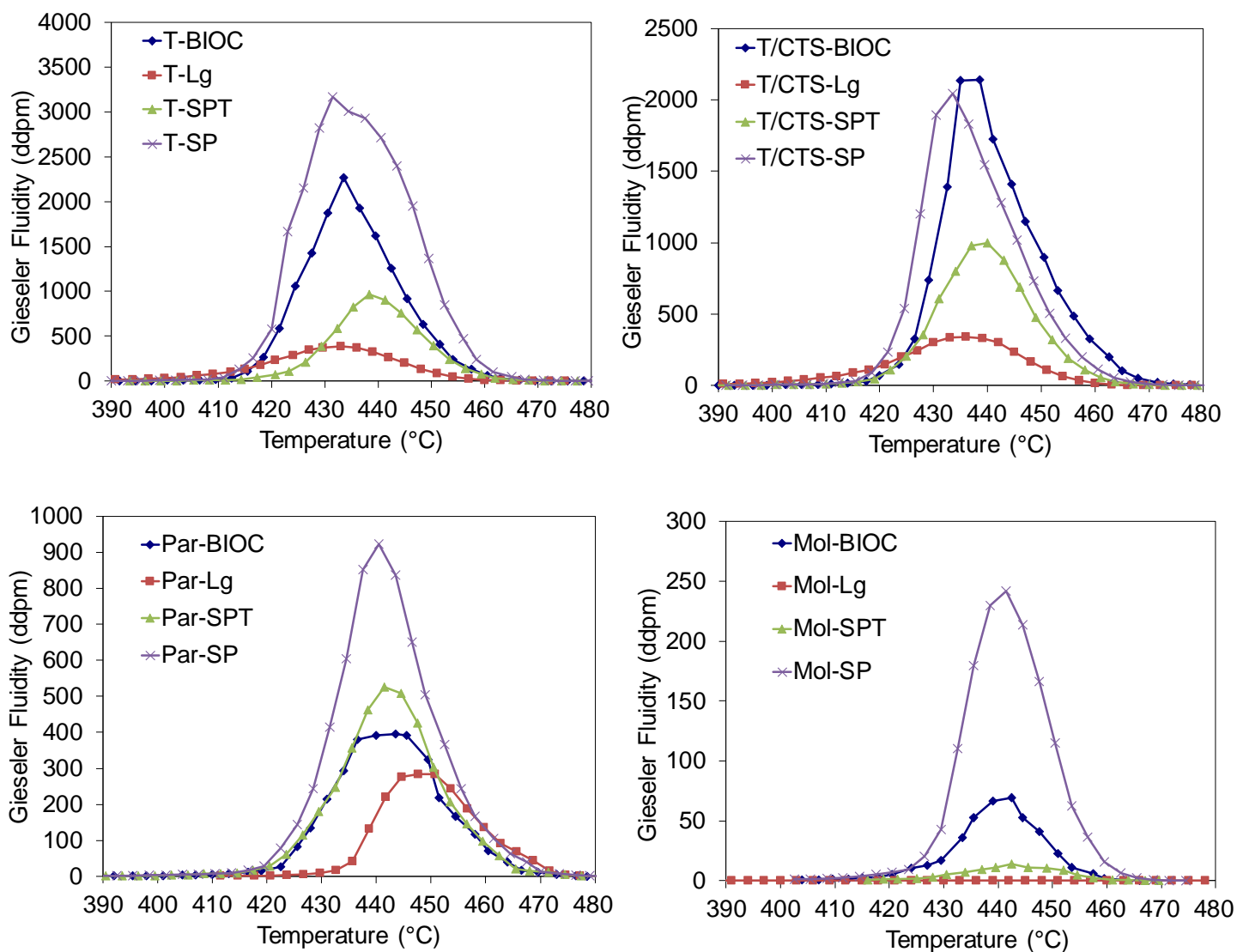


Figure 7. Gieseler fluidity curves as a function of temperature for the briquette blends.

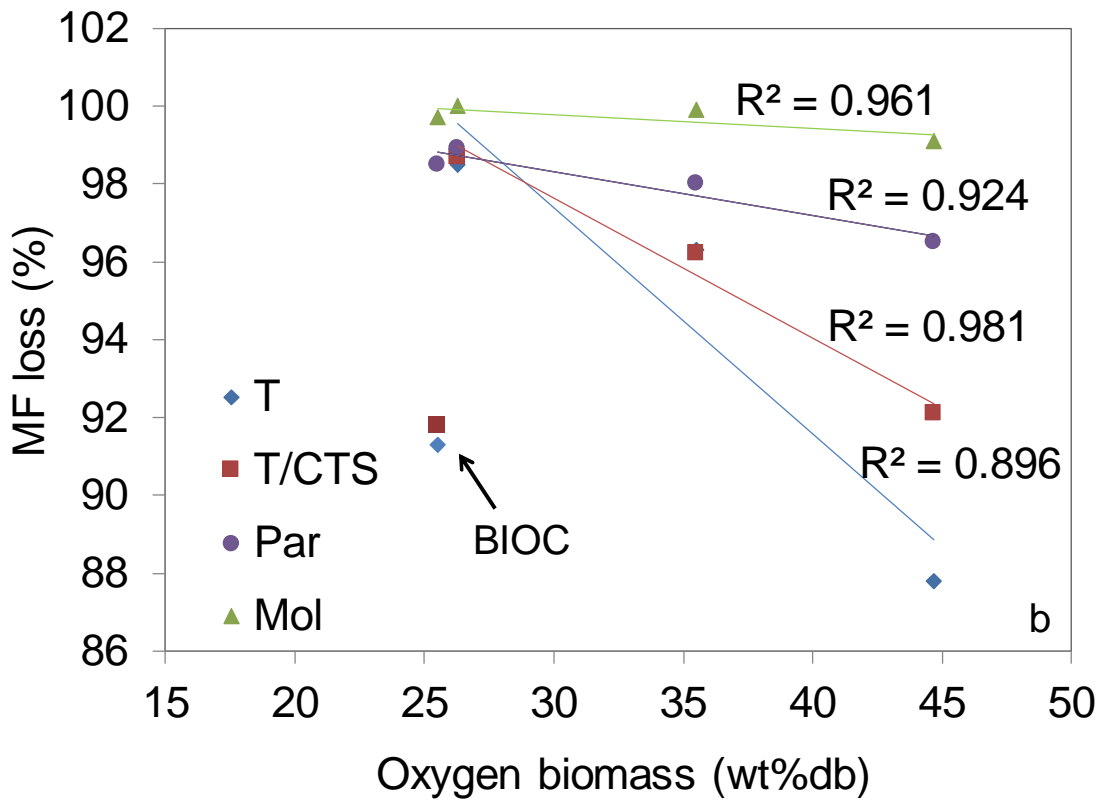
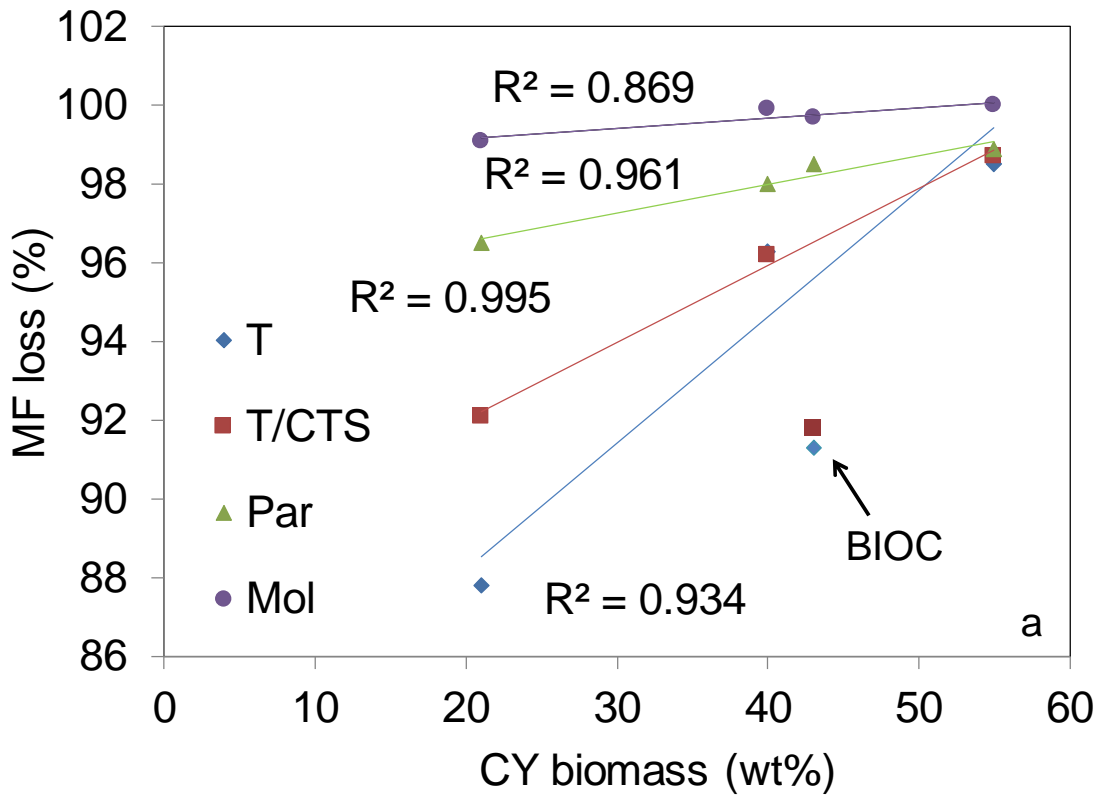


Figure 8. Variation of maximum fluidity loss with a) biomass char yield, from left to right SP, SPT, BIOC and Lg and b) oxygen content of the biomass samples, from left to right BIOC, Lg, SPT and SP.

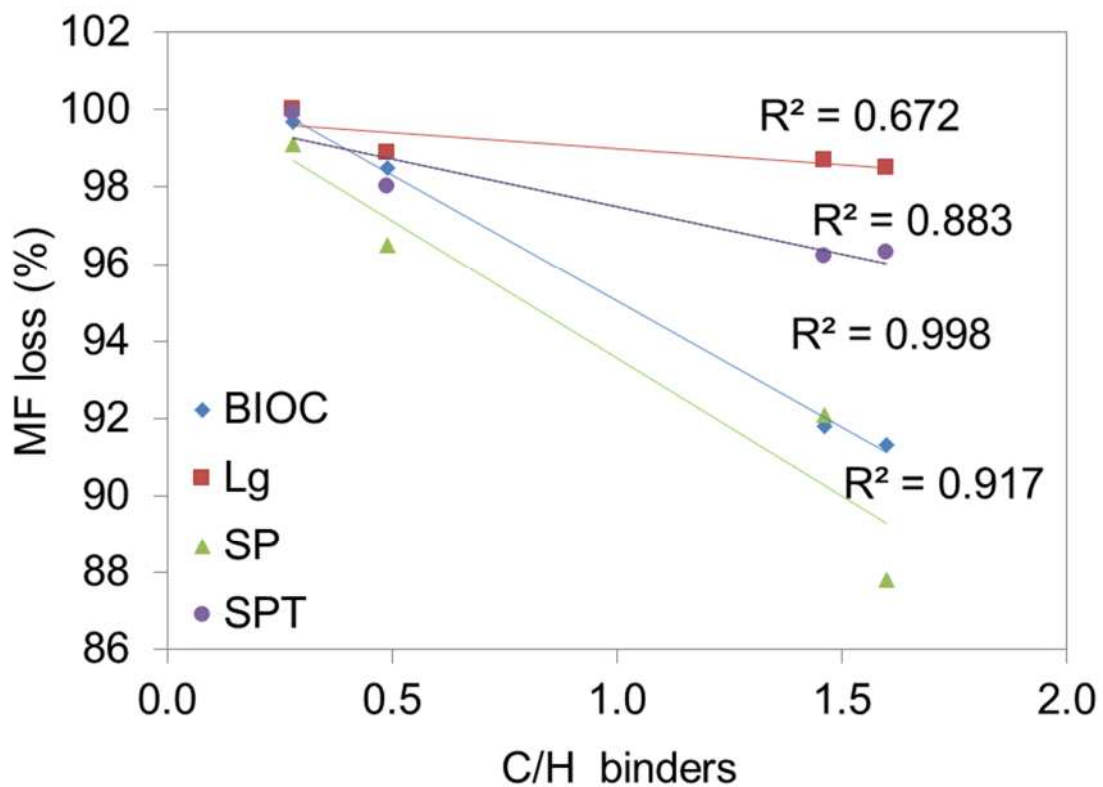


Figure 9. Relationship between the MF loss and the C/H atomic ratio of the binders.  
Binders from left to right: Mol, Par, T/CTS and T.